

1 Technical Note

2

3 Title:

4 Modelling the stance leg in 2D analyses of sprinting: inclusion of the MTP joint affects joint  
5 kinetics (corrected version)

6

7 Authors:

8 Neil E. Bezodis<sup>a,b</sup>, Aki I.T. Salo<sup>b</sup>, Grant Trewartha<sup>b</sup>

9 bezodisn@smuc.ac.uk.

10 A.Salo@bath.ac.uk

11 G.Trewartha@bath.ac.uk

12

13 Affiliations:

14 <sup>a</sup>School of Sport, Health and Applied Science, St Mary's University College, Twickenham, UK.

15 <sup>b</sup>Sport, Health and Exercise Science, University of Bath, UK.

16

17 Keywords:

18 Biomechanics, foot model, joint moments, metatarsal-phalangeal, sprint start

19

20 Abstract

21 Two-dimensional analyses of sprint kinetics are commonly undertaken but often ignore the  
22 metatarsal-phalangeal (MTP) joint and model the foot as a single segment. The aim of this  
23 study was to quantify the role of the MTP joint in the early acceleration phase of a sprint and to  
24 investigate the effect of ignoring the MTP joint on the calculated joint kinetics at the other stance  
25 leg joints. High-speed video and force platform data were collected from four to five trials for  
26 each of three international athletes. Resultant joint moments, powers and net work at the stance  
27 leg joints during the first stance phase after block clearance were calculated using three  
28 different foot models. Considerable MTP joint range of motion ( $>30^\circ$ ) and a peak net MTP  
29 plantar flexor moment of magnitude similar to the knee joint were observed, thus highlighting the  
30 need to include this joint for a more complete picture of the lower limb energetics during early  
31 acceleration. Inclusion of the MTP joint had minimal effect on the calculated joint moments, but  
32 some of the calculated joint power and work values were significantly ( $P < 0.05$ ) and  
33 meaningfully affected, particularly at the ankle. The choice of foot model is therefore an  
34 important consideration when investigating specific aspects of sprinting technique.

35

## 36 Introduction

37 Biomechanists often develop linked-segment rigid body models comprising the segments and  
38 joints deemed to be of sufficient importance to an activity of interest. When joint kinetics are also  
39 required, these models are typically incorporated within inverse dynamics analyses (IDA). The  
40 lower limb joint moments in sprinting have been widely investigated using IDA to understand the  
41 two-dimensional (2D) sagittal plane movements occurring in the primary plane (e.g. Mann,  
42 1981; Jacobs & van Ingen Schenau, 1992; Johnson & Buckley, 2001; Kuitunen et al., 2002;  
43 Hunter et al., 2004; Mero et al., 2006; Bezodis et al., 2008). These studies all used a three  
44 segment representation of the leg which included thigh, shank and foot segments. Whilst the  
45 thigh and shank segments were consistently modelled from hip to knee, and knee to ankle joint  
46 centres, respectively, some of these studies modelled the foot from the ankle to the distal hallux,  
47 and others to the metatarsal-phalangeal (MTP) joint. Kinematic 2D analyses of sprinting have  
48 revealed that rotation in excess of 20° occurs about the MTP joint (Stefanyshyn & Nigg, 1997;  
49 Krell & Stefanyshyn, 2006; Toon et al., 2009); by ignoring this motion any resultant joint  
50 moments generated about the MTP joint, and their consequent effects, are also ignored.

51  
52 Since Elftman (1940) proposed that the resultant moments about the MTP joint are large  
53 enough to warrant consideration in sprint analyses, it appears that only Stefanyshyn & Nigg  
54 (1997) have included an MTP joint when calculating 2D joint kinetics during sprinting.  
55 Stefanyshyn & Nigg (1997) observed peak resultant MTP plantarflexor moments of up to  
56 120 N·m (at the 15 m mark), and up to 70 J of energy was found to be absorbed at the MTP  
57 joint, accounting for around 32% of the total energy absorbed in the four leg joints (MTP, ankle,  
58 knee, hip) during ground contact. These results suggest that it could be important to include the  
59 MTP joint when conducting a sprint-related IDA, but the extent to which this would affect the  
60 calculated kinetics at the other joints in the leg model is not clear. Whilst using different distal  
61 endpoints for a single foot segment could slightly affect the magnitude of the calculated

62 resultant joint moments in the stance leg, it is proposed that ignoring the MTP joint will have a  
63 more pronounced effect. The aim of this study was thus to investigate the effect of three  
64 different foot models on leg joint kinetics during a stance phase in sprinting.

65

## 66 Methods

67 A single-subject approach was adopted since the foot models may affect the joint kinetics on an  
68 individual basis. However, to widen the potential application of the findings, this within-subject  
69 analysis was repeated across three relatively heterogeneous trained athletes (Table 1).  
70 Following ethical approval and written informed consent, a high-speed digital video camera  
71 (Motion Pro<sup>®</sup>, HS-1, Redlake, USA; 200 Hz) was used to capture full body sagittal plane  
72 kinematic data during the first stance phase of maximal effort sprints to 30 m on an indoor track  
73 as a part of larger research study. The camera was positioned 25.00 m away from the centre of  
74 the running lane, perpendicular to the direction of the sprint, 0.95 m in front of the start line and  
75 with the lens centre 1.00 m above the ground. An area of 2.000 m horizontally × 1.600 m  
76 vertically was calibrated, and the camera collected images at a resolution of 1280 × 1024 pixels  
77 with a 1/1000 s shutter speed. A start line was positioned on the track such that the first foot  
78 contact would occur near the centre of a 0.900 × 0.600 m covered force platform (Kistler,  
79 9287BA, Kistler Instruments Ltd., Switzerland; 1000 Hz) embedded in the track. Each trial was  
80 initiated by a trigger button which activated a sounder (to which the athletes reacted), the force  
81 platform, and a series of 20 LEDs (Wee Beasty Electronics, UK) to allow synchronisation of the  
82 video and ground reaction force (GRF) data to the nearest 1 ms.

83

84 \*\*\*\*Table 1 near here\*\*\*\*

85

86 From the video files, six points (shoulder, stance hip, knee, ankle and mid MTP joint centres,  
87 and distal hallux) were manually digitised and affine scaled from 10 frames prior to touchdown

88 until 10 frames after toe-off (Peak Motus<sup>®</sup>, v. 8.5, Vicon, USA). It has previously been proposed  
89 that displacement and force data used for IDA should be subjected to the same level of  
90 smoothing to prevent artificial impact joint moments being introduced (van den Bogert & de  
91 Koning, 1996; Bisseling & Hof, 2006). The displacement and GRF data were therefore passed  
92 through a fourth-order Butterworth filter using the mean optimal cut-off frequency (24 Hz)  
93 determined from a residual analysis of all displacement data (Winter, 1990).

94

95 To create the experimental conditions, the stance leg was represented using three different  
96 models (Figure 1). The thigh and shank segments were consistently modelled from hip to knee,  
97 and knee to ankle joint centres, respectively. For two of the models, the foot was modelled as a  
98 single segment, firstly from ankle to distal hallux (model 3segH) and secondly from ankle to  
99 MTP (3segM). The final model (4seg) included a two segment foot, comprising a rearfoot  
100 segment from ankle to MTP and a forefoot segment from MTP to distal hallux. Individual-  
101 specific segmental inertia data were obtained using the model of Yeadon (1990), which  
102 provided appropriate data for the foot in all three models. To account for the spiked shoes,  
103 0.20 kg was added to the mass of the foot (e.g. Hunter et al., 2004). For model 4seg, this was  
104 divided between the segments based on the ratio of forefoot:rearfoot length. Joint angles were  
105 determined, and were subjected to second central difference calculations (Miller & Nelson,  
106 1973) to derive corresponding velocity and acceleration time-histories.

107

108 \*\*\*\*Figure 1 near here\*\*\*\*

109

110 Prior to filtering, the raw GRF data were downsampled to 200 Hz, and centre of pressure data  
111 were calculated accounting for the thickness of the track surface. These downsampled GRF  
112 data were combined with the kinematic and inertia data in an IDA (Elftman, 1939; Winter, 1990).  
113 Since contact only occurred with the forefoot segment during this early part of a sprint for these

114 three sprinters, all calculations started with the GRF being applied at the centre of pressure to  
115 the most distal segment and proceeded in a distal-to-proximal fashion (i.e. there was no need to  
116 share the GRF between the forefoot and rearfoot in model 4seg). Contact with only the forefoot  
117 was confirmed as a normal occurrence during the first stance phase of a sprint through an  
118 additional qualitative analysis of the 13 University-level sprinters studied by Bezodis et al.  
119 (2010). Joint power was calculated as the product of resultant moment and angular velocity, and  
120 net joint work was calculated as the time-integral of power. For all calculated variables,  
121 extension/plantarflexion was defined as positive. Mean and standard deviations were calculated  
122 for all variables for each athlete. Repeated measures ANOVA comparisons (SPSS 15.0 for  
123 Windows, SPSS Inc., USA) were run for dependent variables (peak resultant extensor joint  
124 moments and powers, and net joint work) for all three athletes separately. When a significant ( $P$   
125  $< 0.05$ ) main effect was observed, Bonferroni *post hoc* tests were calculated to investigate the  
126 pairwise differences.

127

## 128 Results

129 The mean horizontal velocity of the athletes at touchdown was  $3.29 \pm 0.22$  m/s, and during the  
130 first stance phase (mean duration =  $0.188 \pm 0.009$  s), velocity increased by  $1.27 \pm 0.11$  m/s. The  
131 MTP angle ranges of motion during stance for athletes A, B, and C were  $34 \pm 7^\circ$ ,  $30 \pm 7^\circ$ , and  
132  $31 \pm 1^\circ$ , respectively. Time histories for MTP joint angle, angular velocity, resultant moment, and  
133 power from model 4seg are presented in Figure 2. To illustrate the general temporal patterns of  
134 the joint kinetic data during stance when using each of the three leg models, Figure 3 presents  
135 the mean resultant moment and power time histories for the ankle, knee, and hip joints for  
136 athlete C. Differences between leg models were essentially non-existent when considering joint  
137 moment patterns at the ankle, knee and hip joints (some significant differences were observed  
138 due purely to the systematic nature of these small effects; Table 2). However, some significant  
139 and more meaningful differences were observed in joint power and work values due to

140 variations in the calculated angular velocity data between leg models, particularly at the ankle  
141 joint.

142

143 \*\*\*\*Figures 2a-d near here\*\*\*\*

144 \*\*\*\*Table 2 near here\*\*\*\*

145 \*\*\*\*Figures 3a-f near here\*\*\*\*

146

147 Discussion

148 The MTP joint rotated through mean ranges of motion in excess of 30° for each of the three  
149 athletes (Figure 2a), similar to previous results (Krell & Stefanyshyn, 2006; Toon et al., 2009).

150 The mean peak MTP resultant joint moments ranged from 67 to 143 N·m (1.1–1.7 N·m/kg;

151 Figure 2c), and are due to both the biological structures crossing the MTP joint and to the

152 spiked shoe (Oleson et al., 2005). Due to these moments and the observed angular velocities

153 (Figure 2b), the MTP joint is clearly important in absorbing energy during the stance phase

154 (Figure 2d), reaching magnitudes of up to 50 J for some trials of athlete C (Table 2). For

155 athletes A and B in particular, the magnitudes of the resultant joint moments, power and net

156 work at the MTP joint were comparable to those of the knee joint, and it therefore appears

157 important to include this joint in analyses of the energetics of sprinting to obtain a more

158 complete understanding of the internal kinetics. Although there were systematic and statistically

159 significant differences in ankle and hip joint moment (Table 2), these were very small in

160 magnitude (typically less than 1 Nm at the ankle joint). When placed in the context of the typical

161 within-athlete variation based on the standard deviation data presented in Table 2, the practical

162 significance of these differences due to the choice of leg model is clearly minimal, opposing the

163 suggestion in our original paper (Bezodis et al., 2012). The observed significant differences in

164 ankle joint work and power (Table 2 and Figure 3b) between the models which linked the ankle

165 to the MTP joint (3segM and 4seg) and the model which linked the ankle to the distal hallux

166 (3segH) are more practically meaningful. These differences can be attributed to contrasting  
167 ankle joint angular velocities between these two three-segment leg models, and they highlight  
168 that the choice of distal endpoint for a single segment foot could influence the results if absolute  
169 values of ankle joint power or work are of interest.

170

171 The foot is clearly multisegmental and three dimensional, and while inclusion of the MTP joint  
172 reveals 'within-foot' energetics that would be overlooked if using a single-segment  
173 representation, it is acknowledged that it remains a simplification. However, coaches and  
174 biomechanists are often interested in the 2D mechanics of sprinting (e.g., Mann, 1981; Jacobs  
175 & van Ingen Schenau, 1992; Johnson & Buckley, 2001; Kuitunen et al., 2002; Hunter et al.,  
176 2004; Mero et al., 2006; Bezodis et al., 2008) due to the largely planar nature of the skill in  
177 addition to time and equipment/instrumentation constraints.

178

179 The results of the current study revealed that the resultant joint moments, power and net work at  
180 the MTP joint are large enough to warrant consideration in future kinetic analyses of early  
181 acceleration. Due to the increased requirement for energy absorption combined with the  
182 considerable motion previously observed at the MTP joint during maximum velocity sprinting  
183 (Krell and Stefanyshyn, 2006), it is likely that the MTP joint should be considered in kinetic  
184 analyses throughout all phases of a sprint. However, if the specific kinetics of just the ankle,  
185 knee and/or hip joint are the sole focus of a study, a three segment leg model will yield  
186 appropriate data providing that the MTP joint is used as the distal endpoint for the foot segment  
187 if ankle joint power or work data are of interest.

188

189 Acknowledgements

190 The authors are grateful to the University of Wales Institute, Cardiff and the National Indoor  
191 Athletics Centre for providing facilities for data collection. Dr Ian Bezodis is thanked for his  
192 assistance in relation to the data collection.

193

194

## 195 References

196 Bezodis, I. N., Kerwin, D. G., & Salo, A. I. T. (2008). Lower-limb mechanics during the support  
197 phase of maximum-velocity sprint running. *Medicine and Science in Sports and Exercise*, *40*,  
198 707-715.

199

200 Bezodis, N. E., Salo, A. I. T., & Trewartha, G. (2010). Choice of sprint start performance  
201 measure affects the performance-based ranking within a group of sprinters: which is the most  
202 appropriate measure? *Sports Biomechanics*, *9*, 258-269.

203

204 Bisseling, R. W., & Hof, A. L. (2006). Handling of impact forces in inverse dynamics. *Journal of*  
205 *Biomechanics*, *39*, 2438-2444.

206

207 van den Bogert, A. J., & de Koning, J. J. (1996). On optimal filtering for inverse dynamics  
208 analysis. In J. A. Hoffer, A. Chapman, J. J. Eng, A. Hodgson, T. E. Milner & D. Sanderson  
209 (Eds.), *Proceedings of the IX<sup>th</sup> Biennial Conference of the Canadian Society for Biomechanics*  
210 (pp. 214-215). Vancouver: University Press.

211

212 Elftman, H. (1939). Forces and energy changes in the leg during walking. *American Journal of*  
213 *Physiology*, *125*, 339-356.

214

215 Elftman, H. (1940). The work done by muscles in running. *American Journal of Physiology*, 129,  
216 672-684.

217

218 Hunter, J. P., Marshall, R. N., & McNair, P. J. (2004). Segment-interaction analysis of the stance  
219 limb in sprint running. *Journal of Biomechanics*, 37, 1439-1446.

220

221 Jacobs, R., & van Ingen Schenau, G. J. (1992). Intermuscular coordination in a sprint push-off.  
222 *Journal of Biomechanics*, 25, 953-965.

223

224 Johnson, M. D., & Buckley, J. G. (2001). Muscle power patterns in the mid-acceleration phase  
225 of sprinting. *Journal of Sports Sciences*, 19, 263-272.

226

227 Krell, J. B., & Stefanyshyn, D. J. (2006). The relationship between extension of the  
228 metatarsophalangeal joint and sprint time for 100 m Olympic athletes. *Journal of Sports  
229 Sciences*, 24, 175-180.

230

231 Kuitunen, S., Komi, P. V., & Kyröläinen, H. (2002). Knee and ankle joint stiffness in sprint  
232 running. *Medicine and Science in Sports and Exercise*, 34, 166-173.

233

234 Mann, R. V. (1981). A kinetic analysis of sprinting. *Medicine and Science in Sports and  
235 Exercise*, 13, 325-328.

236

237 Mero, A., Kuitunen, S., Harland, M., Kyröläinen, H., & Komi, P. V. (2006). Effects of muscle-  
238 tendon length on joint moments and power during sprint starts. *Journal of Sports Sciences*, 24,  
239 165-173.

240

241 Miller, D., & Nelson, R. (1973). *Biomechanics of sport: a research approach*. Philadelphia, PA:  
242 Lea & Febiger.  
243  
244 Oleson, M., Adler, D., & Goldsmith, P. (2005). A comparison of forefoot stiffness in running and  
245 running shoe bending stiffness. *Journal of Biomechanics*, 38, 1886-1894.  
246  
247 Stefanyshyn, D. J., & Nigg, B. M. (1997). Mechanical energy contribution of the  
248 metatarsophalangeal joint to running and sprinting. *Journal of Biomechanics*, 30, 1081-1085.  
249  
250 Stefanyshyn, D. J., & Nigg, B. M. (2000). Influence of midsole bending stiffness on joint energy  
251 and jump height performance. *Medicine and Science in Sports and Exercise*, 32, 471-476.  
252  
253 Toon, D., Williams, B., Hopkinson, N., & Caine, M. (2009). A comparison of barefoot and sprint  
254 spike conditions in sprinting. *Journal of Sports Engineering and Technology*, 223, 77-87.  
255  
256 Winter, D. A. (1990). *Biomechanics and motor control of human movement*. New York: Wiley.  
257  
258 Yeadon, M. R. (1990). The simulation of aerial movement-II: a mathematical inertia model of the  
259 human-body. *Journal of Biomechanics*, 23, 67-74.  
260

261 Table 1. Descriptive characteristics for the three athletes.

	A	B	C
Age [years]	26	21	20
Gender	Female	Male	Male
Mass [kg]	60.5	82.6	86.9
Height [m]	1.76	1.81	1.78
PB [s]	12.72 <sup>#</sup>	10.14 <sup>*</sup>	10.28 <sup>*</sup>
No. of trials	4	5	5

262 <sup>#</sup> indicates personal best (PB) for 100 m hurdles; <sup>\*</sup> indicates PB for 100 m; A: World Indoor  
263 Championships medalist; B: European Indoor Championships medalist; C: European Indoor  
264 Championships finalist

265  
266

Table 2. Peak resultant joint moments and powers, and net work, for each of the three athletes using each of the three leg models (mean  $\pm$  s).

	Athlete	3segH	3segM	4seg
Peak resultant MTP joint extensor moment [N·m]	A			67 $\pm$ 6
	B			107 $\pm$ 5
	C			143 $\pm$ 8
Peak resultant ankle joint extensor moment [N·m]	A*	210 $\pm$ 9 <sup>b,c</sup>	210 $\pm$ 9 <sup>a,c</sup>	210 $\pm$ 9 <sup>a,b</sup>
	B*	351 $\pm$ 19 <sup>b,c</sup>	351 $\pm$ 19 <sup>a,c</sup>	351 $\pm$ 19 <sup>a,b</sup>
	C*	363 $\pm$ 6 <sup>b,c</sup>	364 $\pm$ 6 <sup>a,c</sup>	364 $\pm$ 6 <sup>a,b</sup>
Peak resultant knee joint extensor moment [N·m]	A	75 $\pm$ 14	75 $\pm$ 14	75 $\pm$ 14
	B	67 $\pm$ 21	66 $\pm$ 22	66 $\pm$ 22
	C	172 $\pm$ 18	172 $\pm$ 18	172 $\pm$ 19
Peak resultant hip joint extensor moment [N·m]	A	137 $\pm$ 14	136 $\pm$ 14	136 $\pm$ 14
	B*	237 $\pm$ 56 <sup>c</sup>	245 $\pm$ 53	247 $\pm$ 53 <sup>a</sup>
	C*	264 $\pm$ 33	266 $\pm$ 32	262 $\pm$ 31
Peak positive MTP joint power [W]	A			253 $\pm$ 106
	B			612 $\pm$ 418
	C			219 $\pm$ 109
Peak positive ankle joint power [W]	A	2177 $\pm$ 326	2228 $\pm$ 260	2221 $\pm$ 259
	B*	2629 $\pm$ 236 <sup>b,c</sup>	2970 $\pm$ 189 <sup>a,c</sup>	2963 $\pm$ 188 <sup>a,b</sup>
	C*	3378 $\pm$ 83 <sup>b,c</sup>	3891 $\pm$ 79 <sup>a,c</sup>	3881 $\pm$ 79 <sup>a,b</sup>
Peak positive knee joint power [W]	A	423 $\pm$ 28	420 $\pm$ 33	425 $\pm$ 37
	B	383 $\pm$ 200	350 $\pm$ 191	351 $\pm$ 191
	C*	1053 $\pm$ 95 <sup>c</sup>	1051 $\pm$ 96 <sup>c</sup>	1062 $\pm$ 97 <sup>a,b</sup>
Peak positive hip joint power [W]	A	1292 $\pm$ 208	1295 $\pm$ 213	1268 $\pm$ 211
	B*	2980 $\pm$ 696 <sup>c</sup>	3088 $\pm$ 651	3107 $\pm$ 647 <sup>a</sup>
	C*	2853 $\pm$ 479	2868 $\pm$ 472 <sup>c</sup>	2815 $\pm$ 469 <sup>b</sup>
Net MTP joint work [J]	A			-22 $\pm$ 5
	B			-26 $\pm$ 10
	C			-46 $\pm$ 4
Net ankle joint work [J]	A*	49 $\pm$ 9 <sup>b,c</sup>	68 $\pm$ 6 <sup>a,c</sup>	68 $\pm$ 6 <sup>a,b</sup>
	B*	81 $\pm$ 13 <sup>c</sup>	97 $\pm$ 16 <sup>c</sup>	96 $\pm$ 16 <sup>a,b</sup>
	C*	91 $\pm$ 7 <sup>b,c</sup>	127 $\pm$ 9 <sup>a,c</sup>	126 $\pm$ 9 <sup>a,b</sup>
Net knee joint work [J]	A*	20 $\pm$ 13 <sup>b,c</sup>	19 $\pm$ 12 <sup>a</sup>	18 $\pm$ 12 <sup>a</sup>
	B*	-5 $\pm$ 18 <sup>b,c</sup>	-9 $\pm$ 17 <sup>a</sup>	-9 $\pm$ 17 <sup>a</sup>
	C*	82 $\pm$ 17 <sup>b,c</sup>	80 $\pm$ 17 <sup>a</sup>	80 $\pm$ 17 <sup>a</sup>
Net hip joint work [J]	A*	76 $\pm$ 15 <sup>b,c</sup>	78 $\pm$ 15 <sup>a,c</sup>	80 $\pm$ 15 <sup>a,b</sup>
	B*	108 $\pm$ 20 <sup>b,c</sup>	111 $\pm$ 19 <sup>a,c</sup>	114 $\pm$ 19 <sup>a,b</sup>
	C*	111 $\pm$ 22 <sup>b,c</sup>	113 $\pm$ 22 <sup>a,c</sup>	115 $\pm$ 21 <sup>a,b</sup>

267  
268

\* significant effect of leg model ( $P < 0.05$ ); <sup>a</sup> significantly different from 3segH; <sup>b</sup> significantly different from 3segM; <sup>c</sup> significantly different from 4seg.

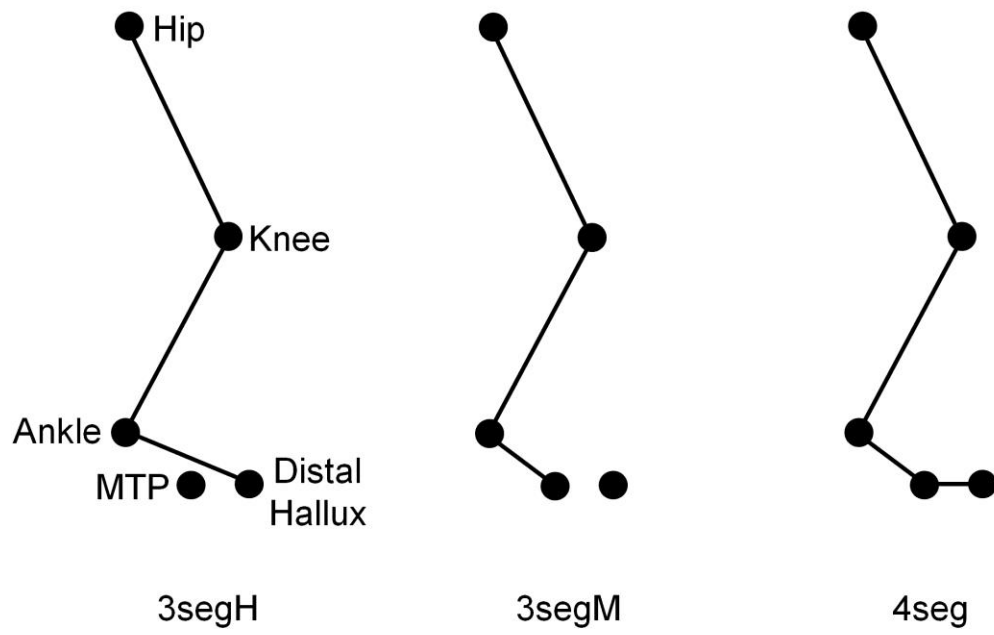
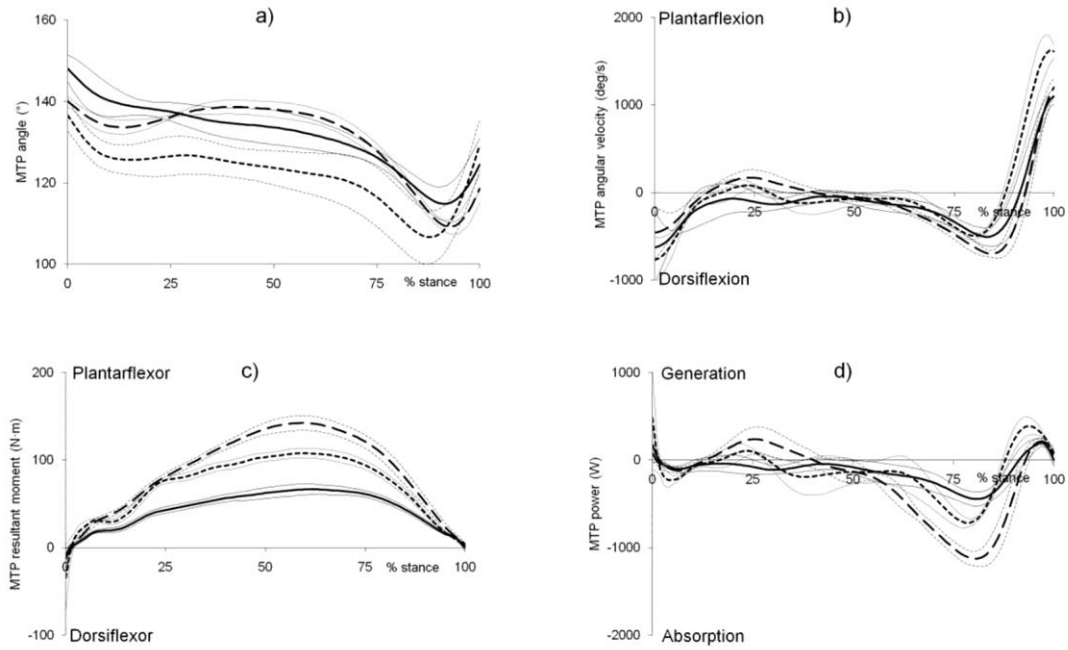


Figure 1. The three models used to represent the stance leg.

269

270



Figures 2a-d. Time-histories (mean  $\pm$  s) for joint angle (a), angular velocity (b), resultant moment (c) and power (d) at the MTP joint during stance for each of the three athletes calculated using the 4seg model (athlete A = solid line, athlete B = dotted line, athlete C = dashed line). MTP joint angle was calculated as the angle between the rearfoot and forefoot segments on the proximal side of the foot.

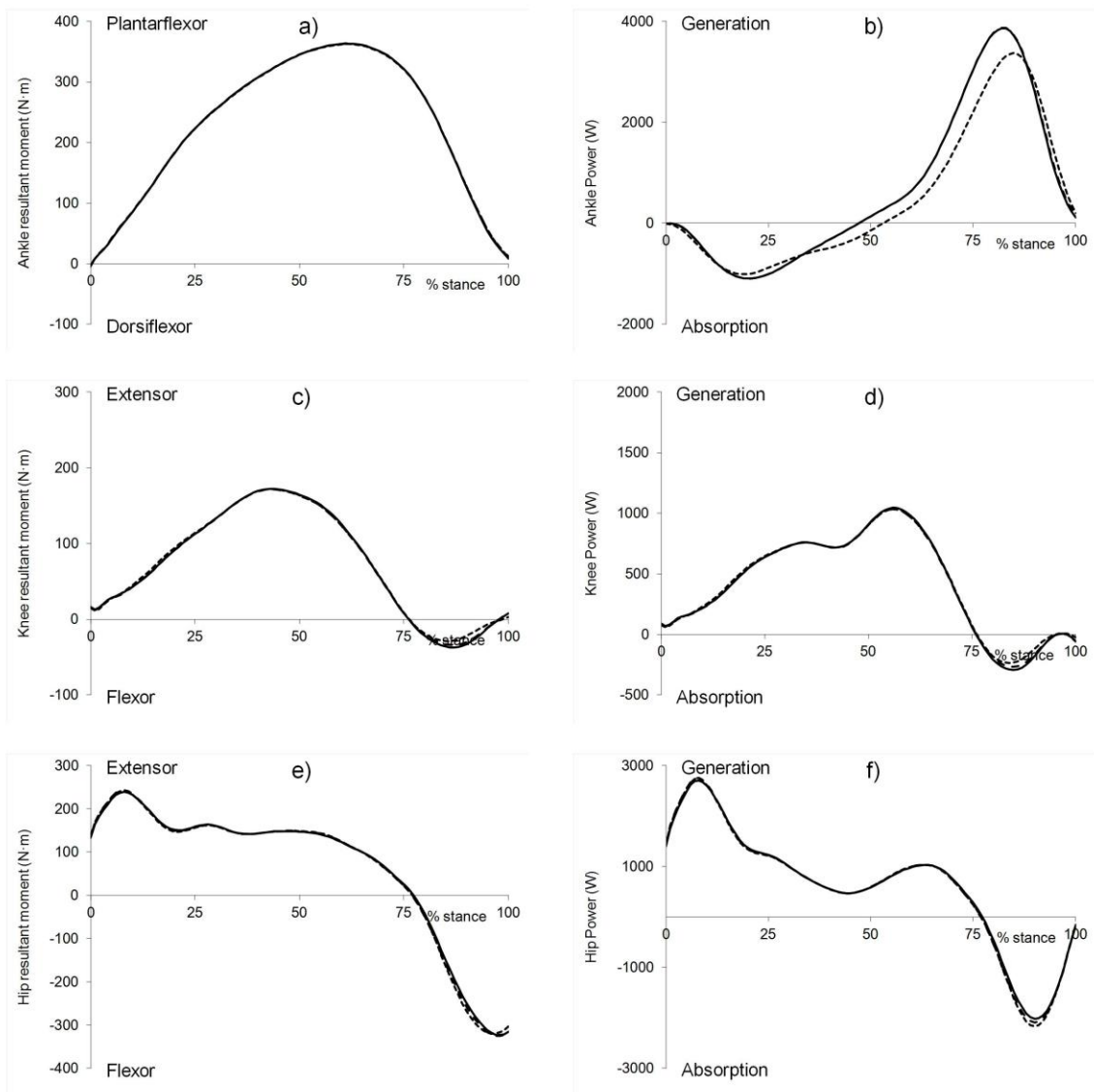


Figure 3. Mean time histories for ankle resultant joint moment (a) and power (b), knee resultant joint moment (c) and power (d), hip resultant joint moment (e) and power (f) for athlete C (model 4seg = solid line, 3segH = dotted line, 3 segM = dashed line).